IEEE Photonics Journal
An IEEE Photonics Society Publication

Open Access

Dielectric Resonator Nanoantenna Coupled to Metallic Coplanar Waveguide

Volume 7, Number 1, February 2015

Gilliard N. Malheiros-Silveira
Hugo E. Hernandez-Figueroa, Senior Member, IEEE

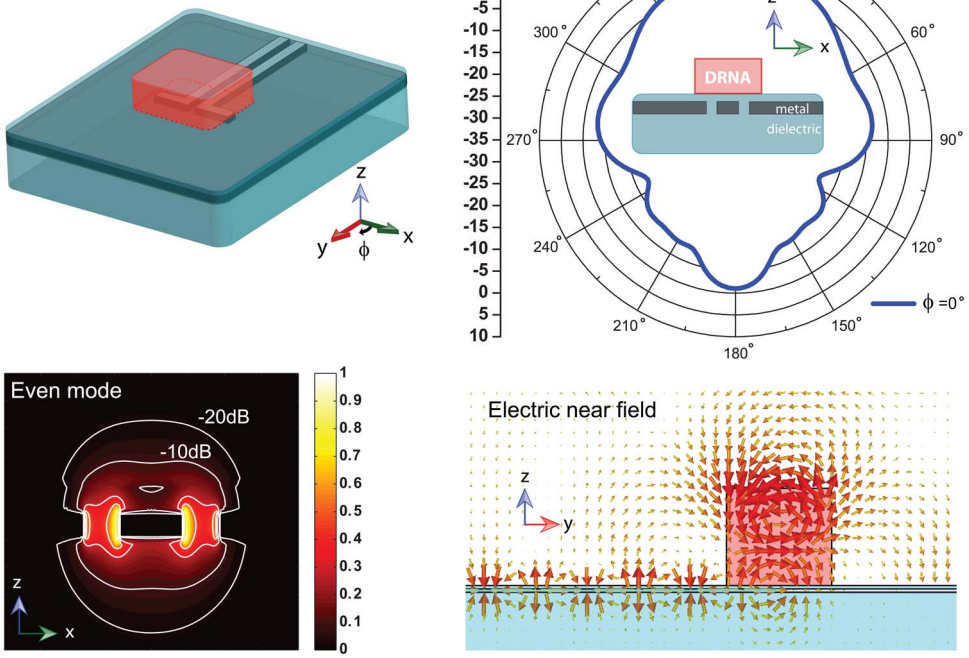

DOI: 10.1109/JPHOT.2015.2399353
1943-0655 © 2015 IEEE

IEEE photonics SOCIETY

IEEE

Dielectric Resonator Nanoantenna Coupled to Metallic Coplanar Waveguide

Gilliard N. Malheiros-Silveira and
Hugo E. Hernandez-Figueroa, *Senior Member, IEEE*

Department of Communications, School of Electrical and Computer Engineering,
University of Campinas, 13083-852 Campinas-SP, Brazil

DOI: 10.1109/JPHOT.2015.2399353

Manuscript received December 28, 2014; revised January 23, 2015; accepted January 27, 2015. Date of publication February 4, 2015; date of current version February 16, 2015. This work was supported in part by São Paulo Research Foundation (FAPESP) under Grant 2010/18857-7 and Grant 2013/03947-9 and in part by the INCT FOTONICOM/CNPq/FAPESP. Corresponding author: G. N. Malheiros-Silveira (e-mail: gnmsilveira@gmail.com).

Abstract: A proposal about a dielectric resonator nanoantenna applied to couple optical beams to a surface plasmon coplanar waveguide (SP CPW), and *vice versa,* was theoretically investigated. The effects of this device operating in optical frequencies were studied, taking into account the central frequency of the conventional optical communication spectrum (C-band). Numerical results show that this proposal is interesting in that it couples an optical beam with an SP CPW with a good reflection coefficient, gain, and broadside radiation pattern.

Index Terms: Nanoantennas, plasmonics, optical resonators, dielectric resonator.

1. Introduction

Efficient excitation of plasmonic waveguides from optical beams is a challenging issue which was recently addressed by means of the nanoantenna paradigm [1], [2]. However, most of the proposals used metallic nanoantennas to excite optical transmission lines [3] or plasmonic gap waveguides [4], and to the best of our knowledge, proposals for exciting surface plasmon coplanar waveguide (SP CPW) (see Fig. 1) [5] by an optical beam has yet to be done. On the other hand, dielectric resonator nanoantennas (DRNAs) have recently been studied, for example, in reflector antennas [6] and reflector arrays [7], and have been applied to excite plasmonic nanostrip waveguides [8].

In that context, we report a theoretical study in which a DRNA was applied to couple optical beams to a SP CPW and *vice versa*. Fig. 1 illustrates the sketch of a SP CPW cross-section, whose electric fields from its fundamental modes (even and odd) are pointed out in the insets.

2. Design

We start by analyzing some important characteristics of a SP CPW in order to pave a way for modeling its coupling to a DRNA. 2-D modal analysis was carried out by using a finite-element based code to better estimate some fundamental properties of that type of metal waveguide. The metallic regions were composed of Ag, whose permittivity was assumed to be $\varepsilon_m = -129.1 + 3.283j$ at 1.55 μm [9]. The substrate and superstrate (when applied) for general metal-optics

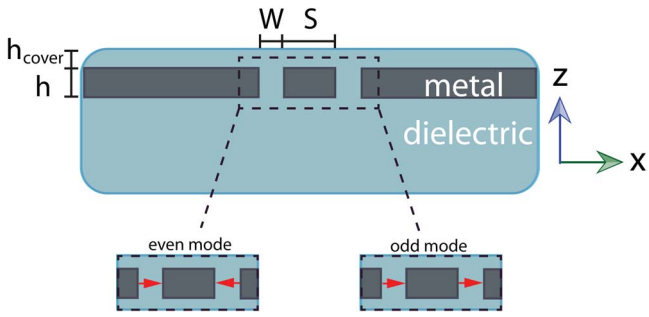

Fig. 1. Cross section view of the assumed SP CPW; blue and dark-gray colors represent dielectric and metal regions, respectively. Arrows in the insets depict the electric field orientation of each fundamental mode.

waveguides are, at the most, composed of low index dielectric material. That region, in this study, was assumed to be composed of SiO_2 ($\varepsilon_r = 2.1$ at 1.55 μm).

Fig. 2 shows the power distribution and effective indexes of both fundamental modes in a SP CPW assuming, arbitrarily, S = 0.090 μm, W = 0.045 μm, h = 0.020 μm, and hcover = 0.020 μm [see Fig. 1] and operating at $\lambda_0 = 1.55$ μm. The cases where the metal that composes that waveguide is Ag [Fig. 2(a)–(c)] or a perfect electric conductor (PEC) [see Fig. 2(d)–(f)] are evaluated in order to point out the similarities/differences between real and ideal metals. Besides that, the approach assuming a PEC is commonly used in designs of coplanar waveguide (CPW) circuits operating in microwaves, where the penetration depth is very low and metal is not so dispersive and lossy as it is in the optical domain.

The similarities are that power has more concentration in the central metal strip for the case of fundamental even modes, and more concentration on the adjacent ones for the case of fundamental odd modes. Furthermore, for both of the cases it was observed that the fundamental modes are quasi-TEM. The calculated skin depth of the Ag [9] at $\lambda_0 = 1.55$ μm is around $\delta = 0.022$ μm. Furthermore, the peak of power is distributed along the gap's edges region for both, even [see Fig. 2(a)] and odd [see Fig. 2(b)] modes) for the metal case. On the other hand, for the PEC case, that peak is mainly concentrated on the gap's corners regions.

Both fundamental modes shown in Fig. 2(c) experience effective indexes higher than the refractive index of the dielectric medium; which indicates that part of those modes are at interface of metal and dielectric, as well as, penetrating inside the metallic region (as previously predicted by the calculation of the skin depth). On the other hand, in Fig. 2(f) the effective indexes for both fundamental modes have lower values than the refractive index of the dielectric medium; which means those modes are mainly leaking at the dielectric region. Taking a look at Fig. 2(d) and (e) it can be observed that power is more confined between the dielectric gaps of the metallic regions than in Fig. 2(a) and (b), respectively. The cases shown in Fig. 2(d)–(f) would represent an equivalent waveguide (but non-plasmonic one) operating in microwaves domain. The fundamental even mode has an effective index higher than the odd one for the swept dimensions shown in Fig. 2(c). As S increases the effective index of the fundamental even mode decreases, whereas the effective index of the odd mode increases; this effect is enhanced as W values decrease. However, in Fig. 2(f) the effective indexes are very low compared to the case of a Drude metal [Fig. 2(c)], besides that, the propagation constants are not so different between themselves and for some specific dimensions those values are equals. Also, as W values increase, the effective index of the even mode become smaller than the odd one.

Assuming the differences and similarities above discussed it is straightforward to expect that a DRNA can operate as a coupling element between SP CPW and an optical beam in a similar way that it occurs in the microwave domain [10]. Next, it will be shown how optical frequencies can affect the performance of this type of antenna.

In order to match a DRNA to a SP CPW, we can assume a linear slot (through the metal region) in a direction perpendicular to the longitudinal direction along the SP CPW. However, a

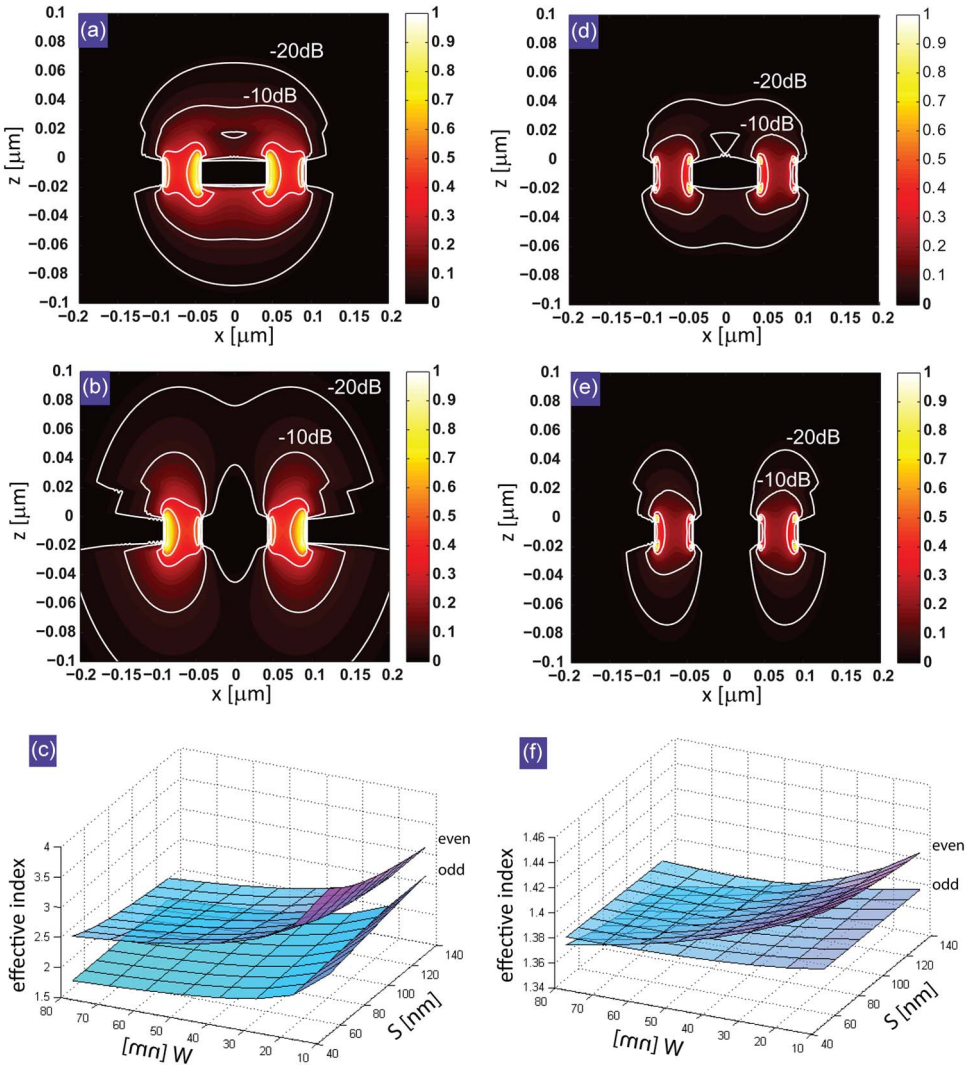

Fig. 2. Longitudinal component of the power flow (time average) in arbitrary normalized units (contour map ranging from light to dark colors represents power's magnitude ranging from high to low values and contours defining regions where power decays to −10 dB and −20 dB are also included) and SP CPW's dimensions (for h = 0.020 μm) versus effective indexes of the fundamental modes at 1.55 μm. Fundamental even mode (a), odd mode (b), and effective indexes variation (c) when Ag is the metal taken into account. Fundamental even mode (d), odd mode (e), and effective indexes variation (f) when PEC is the metal taken into account. The effective indexes for the assumed dimensions are 2.3242 and 1.7652 using Ag for even and odd modes, respectively, and the calculated propagation lengths are 7.39 μm and 11.98 μm, for the fundamental even and odd modes, respectively. By assuming PEC, the fundamental even and odd modes are 1.3763 and 1.3717, respectively.

DRNA with the above-mentioned slot and without a SP CPW is analyzed first in order to evaluate the coupled resonances between the DRNA and that slot. The mentioned set up can be seen in the central inset on top of the Fig. 3. Then, the geometrical parameters for the best case will be assumed in conjunction with a SP CPW.

Although most of the studied DRNAs assume circular cylinder geometry, for example [7], [8], and [11], the geometry of the chosen dielectric resonator element has a rectangular shape. The resonator must be composed of a dielectric material with permittivity higher than the dielectric of the substrate/superstrate in order to efficiently transfer energy from/to the SP CPW. Besides, at the same time that we desire to maintain the generalization, we arbitrarily choose GaAs

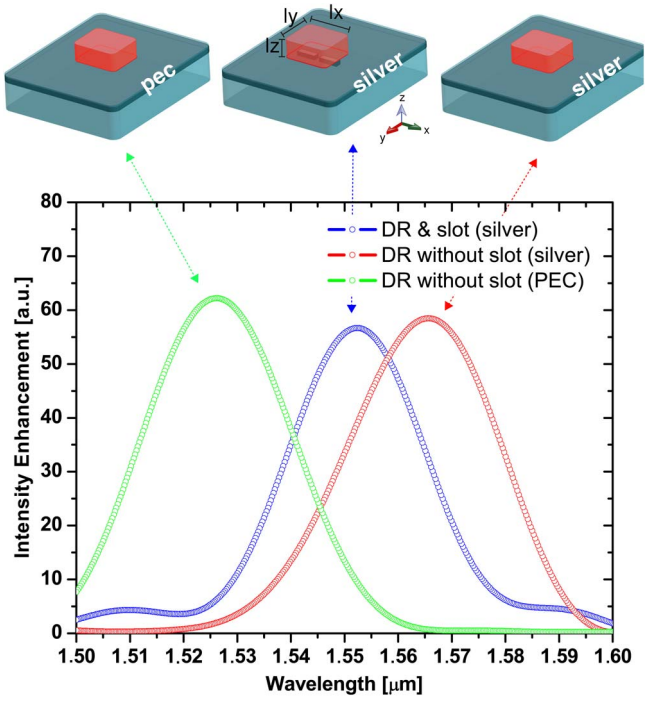

Fig. 3. Resonant wavelength obtained by the peak of intensity enhancement inside the DRNA when TE^x_{113}-like mode is excited from a planewave, E^y polarized and traveling in the -z direction.

($\varepsilon_r = 11.56$ at $\lambda_0 = 1.55$ μm) in order to represent a high index dielectric material. The chosen mode to be excited was a high order TE^x mode, because high-order modes of rectangular dielectric resonator are more directive than the correspondent low-order ones [12]. Furthermore, this type of set up permits the occurrence of only odd modes in the resonator; thus, in order to maintain a reasonable aspect ratio we chose to excite the TE^x_{113} mode. The resonance frequency, f_0, of the TE^x_{113} mode for a rectangular DR, in free space and in the microwave domain, can be estimated from the transcendental equation [13]

$$k_x \tan\left(\frac{k_x l_x}{2}\right) = \sqrt{(\epsilon_r - 1)k_0^2 - k_x^2}, \tag{1}$$

where $k_0 = 2\pi/\lambda_0$, $k_y = \pi/l_y$, $k_z = \pi/l_z$, and $k_x^2 + k_y^2 + k_z^2 = \varepsilon_r k_0^2$. The central inset in Fig. 3 shows the related dimensions of the variables l_x, l_y, and l_z. Also, that mode radiates like a magnetic dipole at the surface of the ground plane and along x direction, plus another one in the upper part of the DR; which can provide a broadside radiation pattern. The radiation Q factor Q_{rad} is given by [13]: $Q_{rad} = 2\omega_0 W_e / P_{rad}$, where ω_0, W_e, and P_{rad} denote the radian resonant frequency, the stored electric energy, and radiated power, respectively. Once that the result from the (1) is related only for the case where the DR is isolated in free space, it will be used as initial value to be optimized by numerical solvers. In order to optimize the DRNA dimensions and the slot ones, which will be used to feed the DRNA, a planewave was assumed traveling in z direction. At this step we account for the dispersive properties of the metal region by using the Drude model

$$\varepsilon_{Ag} = \varepsilon_\infty - f_p^2/[f_0(f_0 + i\gamma)], \tag{2}$$

where $\varepsilon_0 = 8.85 \times 10^{-12}$, $\varepsilon_\infty = 5$, $f_p = 2175$ THz, and $\gamma = 4.35$ THz [14]. Material dispersion can play a strong role in photonics devices; which is not so expressive in the microwave domain.

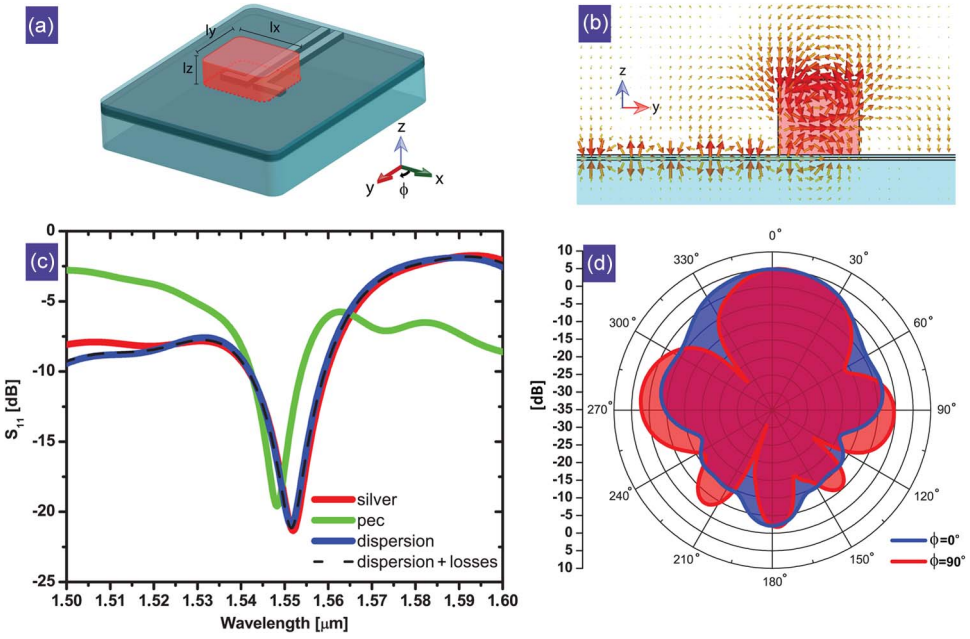

Fig. 4. Fundamental parameters of a DRNA coupled to a SP CPW. (a) Sketch of the DRNA coupled to SP CPW. (b) Electric field distribution of the TE^{x}_{113}-like mode at the plane x = 0. (c) Return loss S_{11} in blue solid line represents the case where dielectric dispersion and Drude metal were assumed. Red line is for the case when just Drude metal was assumed (without dielectric dispersion and losses). Black dashed line represents the case where dielectric and metal dispersion, as well as dielectric losses, were assumed. (Green line) Case when a PEC was assumed. (d) 2-D radiation pattern at $\lambda_0 = 1.55$ μm.

Thus, Sellmeier's equation was used to take dielectric dispersions of the substrate/superstrate and resonator into account:

$$n(\lambda) = \sqrt{A + \sum_j \frac{B_j \lambda^2}{C_j - \lambda^2}} \tag{3}$$

where A = 3.5, $B_1 = 7.4969$, $C_1 = 0.4082$, $B_2 = 1.9347$, and $C_2 = 37.17$ are the coefficients for GaAs [15], and A = 1, $B_1 = 0.6961663$, $C_1 = 0.0684043$, $B_2 = 0.4079426$, $C_2 = 0.1162414$, $B_3 = 0.8974794$, and $C_3 = 9.896161$ are the coefficients for SiO_2 [16].

3. Results and Discussion

Fig. 3 shows the intensity enhancement of one ideal case of DRNA with one slot underneath it, as well as a case when the DRNA is over the same region but without the slot. To reduce the number of variables during the optimization process, the slot width was assumed to be the same as slots that compose the SP CPW: W = 0.045 μm. Its total length was initially estimated from the guided wavelength in a slot in an equivalent slot waveguide to be near to $\lambda_g = \lambda_0/n_{eff} = 1.55$ μm/1.97 = 0.787 μm. Thus, for the slot resonating at $\lambda_0 = 1.55$ μm it is expected its length be smaller than the above mentioned value once the high-index material from the DRNA produces the decreasing of λ_g.

The intensity enhancement of the reflected DRNA shown in the central inset, without SP CPW, is depicted by the blue curve, whose peak is close to the desired wavelength. Through this procedure the DR assumed the values of 0.779 μm, 0.660 μm, and 0.610 μm for l_x, l_y, and l_z, respectively, and Q-factor = 91.27. The total length of the slot assumed the valued of 0.560 μm. Since the absorption coefficient, α, in GaAs is very low at 1.55 μm [17], the material loss was assumed negligible. In that case, its Q-factor is equivalent to the radiation Q-factor.

For comparison's sake, the previous structure without slot presented a shift of its intensity peak around a longer wavelength (see the red curve in Fig. 3). The structure such as the previous one, but assuming a PEC had its intensity peak shifted into a shorter wavelength (it is represented for the green curve).

Finally, the slots of the SP CPW were incorporated to the previous design [as shown in Fig. 4(a)] and the nanoantenna was analyzed assuming its operation in transmission mode. The SP CPW was excited from a waveguide port. The electric field distribution from the SP CPW and DRNA, at the plane x = 0, is shown in Fig. 4(b). The TE^{x}_{113}-like mode has been excited on the DRNA within the S_{11} criterion of -10 dB, and besides that, the radiation patterns maintain very uniform shapes with a very directive main lobe and small variation of the realized gain around 6.0 dB.

Its return loss (S_{11}) is shown in Fig. 4(c). The solid line (in blue) represents the case assuming dispersive materials (SiO_2, GaAs, and Ag), which exhibits resonance at $\lambda_0 = 1.55$ μm (193.5 THz) with a pronounced dip of about -22 dB, and an impedance matching bandwidth of 2.16 THz for values lower than -10 dB. Dielectric cavities can have their bandwidth increased and its quality factor decreased as its dielectric constant is reduced, however there is a trade-off for the studied antenna once the dielectric constant decreases, the mode of the resonator becomes less confined and it can reduce the coupling between it and the waveguide. Solid line (in red) represents the case where just the metal dispersion was assumed, and the dielectric materials have their permittivities constant (same values than at $\lambda_0 = 1.55$ μm). By comparing both cases above mentioned, it is clear that material dispersion for dielectric materials has no substantial effect on the design of that type of nanoantenna. Black dashed line represents the case where dielectric and metal dispersions, as well as losses, were assumed. In order to assume the increasing of dielectric losses in GaAs, doping impurities were assumed: a Se concentration of $N \approx 5.4 \times 10^{18}$ cm^{-3} which increases α value to $\alpha \approx 30$ cm^{-1} [17]. However, that doping was not high enough to produce a bandwidth broaden on the DRNA (which is commonly expected in microwaves). Solid line in green color shows the hypothetical case where the metal is a PEC and where the material dispersion was not assumed (again this approach is quite suitable for applications in the microwave domain). One can perceive that this hypothetical case has a qualitative behavior similar to the most realistic one (the former case); that is because penetration of the electric field into metal is weak at $\lambda_0 = 1.55$ μm [18]. On the other hand, in a quantitative approach, the resonances assume distinct values than the more realistic case. This occurred because the metal dispersion and penetration of electric field into the metal region played a strong role (see Fig. 2), once the thickness of the metal layer was smaller than the skin depth. Those are some of the main aspects which make nanoantenna designs somewhat different from their counterpart in RF/microwave domain [19]. The effect of the PEC in the reflector DRNA, shown in Fig. 3 (in green) is similar to the DRNA for SP CPW, shown in Fig. 4(c) (in green); the resonance occurs in shorter wavelengths.

Fig. 4(d) shows a broadside radiation pattern with main lobe direction of $\theta = 0^\circ$ and $\theta = 4^\circ$ for the planes at $\phi = 0^\circ$ and $\phi = 90^\circ$, respectively. It has an angular width (3 dB criterion) of 58.1° and 58.6° for the planes $\phi = 0^\circ$ and $\phi = 90^\circ$, respectively. Similar radiation patterns can be observed at microwave domain when using that mode. Since the length scale of the DRNA is very small, a possible way for exciting it can be by using a highly focused and linearly polarized beam. Furthermore, this type of plasmonic transmission line can require fewer steps of the fabrication process compared to a nanostrip waveguide [8], since only one metal layer is required, instead of two of them. The studied DRNA can be integrated to SP CPW, for example, by similar techniques to those ones used for processing plasmonic crystal defect nanolasers (and assuming those materials) [20]. Other interesting approach for the visible spectrum is assuming the DRNA composed of TiO_2, since that material has a higher refractive index in that range [7].

4. Conclusion

We proposed a way for exciting a particular plasmonic waveguide by applying the nanoantenna concept. It was reported a study of DRNA fed by a SP CPW by means of excitation of a high

order mode on that DRNA: the TE^{x}_{113}-like mode. Beside of a pronounced S_{11} dip (about -22 dB at 1.55 μm) and a high gain (about 6.0 dB), the broadside radiation pattern produced by that mode can be used to couple optical energy from/to a SP CPW. Thus, the DRNA coupled to a SP CPW can be a promising proposal not only for coupling light in/out plasmonic circuits, as well as a possible way to realize inter chip wireless communication assuming plasmonic platforms.

References

[1] P. Biagioni, J.-S. Huang, and B. Hecht, "Nanoantennas for visible and infrared radiation," *Rep. Progr. Phys.*, vol. 75, no. 2, 2012, Art. ID. 024402.

[2] G. N. Malheiros-Silveira, L. H. Gabrielli, C. J. Chang-Hasnain, and H. E. Hernandez-Figueroa, "Breakthroughs in Photonics 2013: Advances in nanoantennas," *IEEE Photon. J.*, vol. 6, no. 2, Apr. 2014, Art. ID. 0700706.

[3] J.-S. Huang, T. Feichtner, P. Biagioni, and B. Hecht, "Impedance matching and emission properties of nanoantennas in an optical nanocircuit," *Nano Lett.*, vol. 9, no. 5, pp. 1897–1902, 2009.

[4] J. Wen, S. Romanov, and U. Peschel, "Excitation of plasmonic gap waveguides by nanoantennas," *Opt. Exp.*, vol. 17, no. 8, pp. 5925–5932, Apr. 2009.

[5] K.-Y. Jung, F. L. Teixeira, and R. M. Reano, "Surface plasmon coplanar waveguides: Mode characteristics and mode conversion losses," *IEEE Photon. Technol. Lett.*, vol. 21, no. 10, pp. 630–632, May 2009.

[6] L. Zou *et al.*, "Efficiency and scalability of dielectric resonator antennas at optical frequencies," *IEEE Photon. J.*, vol. 6, no. 4, Aug. 2014, Art. ID. 4600110.

[7] L. Zou *et al.*, "Dielectric resonator nanoantennas at visible frequencies," *Opt. Exp.*, vol. 21, no. 1, Jan. 2013, Art. ID. 1344.

[8] G. N. Malheiros-Silveira, G. S. Wiederhecker, and H. E. Hernández-Figueroa, "Dielectric resonator antenna for applications in nanophotonics," *Opt. Exp.*, vol. 21, no. 1, Jan. 2013, Art. ID. 1234.

[9] P. B. Johnson and R. W. Christy, "Optical constants of the noble metals," *Phys. Rev. B*, vol. 6, no. 12, pp. 4370–4379, Dec. 1972.

[10] M. S. Al Salameh, Y. M. M. Antar, and G. Seguin, "Coplanar-waveguide-fed slot-coupled rectangular dielectric resonator antenna," *IEEE Trans. Antennas Propag.*, vol. 50, no. 10, pp. 1415–1419, Oct. 2002.

[11] J. A. Schuller and M. L. Brongersma, "General properties of dielectric optical antennas," *Opt. Exp.*, vol. 17, no. 26, Dec. 2009, Art. ID. 24084.

[12] A. Petosa and S. Thirakoune, "Rectangular dielectric resonator antennas with enhanced gain," *IEEE Trans. Antennas Propag.*, vol. 59, no. 4, pp. 1385–1389, Apr. 2011.

[13] R. K. Mongia and A. Ittipiboon, "Theoretical and experimental investigations on rectangular dielectric resonator antennas," *IEEE Trans. Antennas Propag.*, vol. 45, no. 9, pp. 1348–1356, Sep. 1997.

[14] H. Iizuka, N. Engheta, H. Fujikawa, and K. Sato, "Arm-edge conditions in plasmonic folded dipole nanoantennas," *Opt. Exp.*, vol. 19, no. 13, pp. 12 325–12 335, Jun. 2011.

[15] A. H. Kachare, "Refractive index of ion-implanted GaAs," *J. Appl. Phys.*, vol. 47, no. 9, pp. 4209, Sep. 1976.

[16] I. H. Malitson, "Interspecimen comparison of the refractive index of fused silica," *J. Opt. Soc. Amer.*, vol. 55, no. 10, pp. 1205, Oct. 1965.

[17] W. Spitzer and J. Whelan, "Infrared absorption and electron effective mass in n-type gallium arsenide," *Phys. Rev.*, vol. 114, no. 1, pp. 59–63, Apr. 1959.

[18] G. Veronis and S. Fan, "Theoretical investigation of compact couplers between dielectric slab waveguides and two-dimensional metal-dielectric-metal plasmonic waveguides," *Opt. Exp.*, vol. 15, no. 3, pp. 1211–1221, Feb. 2007.

[19] L. Novotny, "Effective wavelength scaling for optical antennas" *Phys. Rev. Lett.*, vol. 98, no. 26, Jun. 2007, Art. ID. 266802.

[20] A. M. Lakhani, M. Kim, E. K. Lau, and M. C. Wu, "Plasmonic crystal defect nanolaser," *Opt. Exp.*, vol. 19, no. 19, pp. 18 237–18 245, Sep. 2011.